IEEE Access
Multidisciplinary | Rapid Review | Open Access Journal

Received December 21, 2018, accepted January 14, 2019, date of publication January 17, 2019, date of current version March 20, 2019.

Digital Object Identifier 10.1109/ACCESS.2019.2893660

Calibration Method Based on the Image of the Absolute Quadratic Curve

WENLEI LIU[1], SENTANG WU[1], XIAOLONG WU[2], AND HONGBO ZHAO[1]
[1]School of Automation Science and Electrical Engineering, Beihang University, Beijing 100191, China
[2]Navigation and Control Technology Institute of NORINCO Group, Beijing 100089, China

Corresponding author: Wenlei Liu (liuwenlei@buaa.edu.cn)

This work was supported by the Industrial Technology Development Program under Grant B1120131046.

ABSTRACT In this paper, a new camera calibration method based on the image of the absolute quadratic curve (IAC) is proposed, and a new target is designed for this method, which is both convenient and flexible. It first extracts the characteristic points and the characteristic lines of the target and finds out the vanishing point and the vanishing line. The radial and tangential distortion coefficients are obtained by using the cross ratio invariance to correct the target image distortion. Then, the four internal parameters of the camera are obtained by IAC. The influence of the skew parameters is ignored. The rotation matrix is then calculated by the orthogonal characteristic of the coordinate system, and the translation vector is calculated by the center coordinates of the camera. In this way, the internal and external parameters of the camera can be obtained. The internal and external parameters are taken as initial values, and the optimal results are obtained by nonlinear optimization using the reprojection method. Finally, the relative position between different target images can be obtained by using the fundamental matrix, namely, the rotation angle. In the process of solving, the normalization method is used to improve the accuracy of data processing. Not requiring any prior information of the camera, the method has a wide range of applications.

INDEX TERMS Camera calibration, image of the absolute quadratic curve (IAC), fundamental matrix, cross ratio invariance, vanishing point, vanishing line, distortion correction.

I. INTRODUCTION

In recent years, with the development of artificial intelligence research, computer vision (such as visual navigation SLAM, 3D reconstruction and augmented reality), as one of the key technologies of artificial intelligence, has garnered increased attention. Nowadays, an increasingly large number of people are studying computer vision, the research is quickly gaining depth, and the application of computer vision in daily life is becoming more and more extensive. Before computer image processing, the most important task is to know the parameters of the camera, including its internal and external parameters. The accuracy of camera calibration will directly affect the accuracy of image processing. The way to calibrate camera parameters quickly and accurately under the condition of unknown camera parameters will be the focus of this paper.

The most commonly used camera calibration method is the vanishing point and the vanishing line method to calibrate. Reference [1] presents a global calibration method for widely distributed cameras based on vanishing features and vanishing line. References [2] and [3] propose a method to self-calibrate dynamically moving and zooming cameras and determine their absolute and relative orientations. References [4] and [5] propose a camera calibration method, which uses the property of the vanishing points. The rotation matrix can be computed by matching the corresponding vanishing points in the two images, and a simple triangulation method can calculate the translation vector. The rotation matrix and the translation vector of the camera, i.e., the external parameters of the camera can be easily found by using the vanishing point and the vanishing line methods. However, the premise of using these methods is based on the knowledge of the internal parameters of the camera, and cannot be solved directly.

Homography is the correspondence between two planes. This property is usually used to calibrate the camera. References [6] and [7] propose a method to achieve both dense 3D reconstruction of the scene and estimation of the camera intrinsic parameters by using coplanarities and other constraints derived from relations between planes in the scene

The associate editor coordinating the review of this manuscript and approving it for publication was Yu ZHANG.

and reflected curves of line lasers captured by a single camera. Reference [8] proposes a novel auto-calibration method, which used three eigenvectors of a plane-induced homography to solve for the image of the absolute conic (IAC). The camera calibration parameters can then be obtained. References [9] and [10] present various self-calibration methods to calibrate the rotating and zooming cameras. These methods make use of the infinite homography constraint, which relates the unknown calibration matrices to the computed inter-image homographies. The internal parameters of the camera can be easily obtained by using plane homography, but if the external parameters of the camera are required, other methods must be used in combination.

References [11]–[13] introduce the multiview geometry and projective geometry in detail, and they played an important role in camera calibration. References [14]–[16] propose a novel contour-based algorithm, which used the epipolar geometry recovered from the image and the properties of mirror reflection. It can reconstruct an arbitrary rigid object without knowing the camera parameters and the mirror poses. References [17] and [18] propose a method of calculating the epipolar geometry from profiles under circular motion. After estimating the epipolar geometry, the Euclidean motion is recovered using the fixed intrinsic parameters of the camera, obtained either from a calibration grid or from self-calibration techniques. Multi view geometry plays an important role in camera calibration and 3D reconstruction. The methods provided in this paper will also use the knowledge of multi view geometry. They provide some theoretical basis for this paper.

It is a widely used method to calibrate the internal and external parameters of the camera by using the outline of the object and the plane mirror. References [19] and [20] propose a method that uses a sequence of images of an object rotating about a single axis and analyzes the projective geometry of the situation. References [21] and [22] address a method of recovering both the intrinsic and extrinsic parameters of a camera from the silhouettes of an object in a turntable sequence. According to the image invariants, the rotation angle and a fixed scalar, the fundamental matrix and the imaged circular points for the turntable plane can be calculated. References [23] and [24] propose a method to recover both the intrinsic and extrinsic parameters of the camera using multiple silhouettes from one single image. It uses the projective properties of epipoles to recover both the imaged circular points and the included angle between two mirrors. References [25] and [26] present a self-calibration method to calculate the focal length, principal point, mirror and camera poses directly from the silhouette outlines of the object and its reflections, which uses five views of an object from two planar mirrors. The calibration method based on plane mirror and rotating target is widely applied and has been researched extensively. However, this method is too dependent on auxiliary calibration equipment, and the calibration method is too cumbersome and practical.

This paper will design a new target to calibrate the internal parameters of the camera, which is convenient and flexible to use. The target can be used for de-distortion processing and camera calibration. Before camera calibration, radial and tangential distortion parameters are obtained by using orthogonal invariance and vanishing points to eliminate target image distortion. The method does not involve the internal parameters of the camera and is easy to realize. The basic idea of camera calibration is to first calibrate the internal parameters of the camera by the image of the absolute quadratic curve (IAC), and then calculate the rotation matrix is calculated by the orthogonal characteristic of the coordinate system. The translation vector is computed from the center of the triangle formed by the three vanishing points of the coordinate axis. Finally, the optimal solution of the camera parameters is obtained by using the reprojection method. Fundamental matrix can be used to calculate the relative position between different target images.

The organizational structure of this article is as follows: Section II introduces the definition and basic principles of this article. Section III introduces the method of camera calibration used in this paper. Section IV analyzes and compares the method using physical experiments. Section V summarizes the methods provided in this paper.

II. NOTATION AND BASIC PRINCIPLES

A. CCD CAMERA

In this paper, we use $x = [u_x, u_y]^{\mathrm{T}}$ and $\boldsymbol{X} = [\mathrm{X}, \mathrm{Y}, \mathrm{Z}]^{\mathrm{T}}$ to represent the point in the 2-D image plane and the 3-D space respectively. $\boldsymbol{u_x}$ and $\boldsymbol{u_y}$ are pixel coordinates in the image coordinate system. X, Y and Z are 3-D space coordinates respectively. The homogenous coordinates of x and $\boldsymbol{X}$ are $\tilde{x} = [x^T, 1]^T, \tilde{X} = [X^T, 1]^T$, respectively.

The projection from the point in 3-D space to 2-D image plane can be expressed as follows:

$$\zeta\tilde{x} = [K|0_{3\times1}]T\tilde{X} = K[R|t]\tilde{X} = KR[I|-C]\tilde{X} = P\tilde{X} \quad (1)$$

$$K = \begin{bmatrix} f_x & s & u_x \\ 0 & f_y & u_y \\ 0 & 0 & 1 \end{bmatrix}, \quad T = \begin{bmatrix} R_{3\times3} & t_{3\times1} \\ 0_{1\times3} & 1 \end{bmatrix}, \; t = -RC \quad (2)$$

where, ζ is a scale factor and f_x and f_y are the equivalent focal lengths. $\boldsymbol{s}$ is the skew parameter. (u_x, u_y) is the main point coordinate. $\boldsymbol{R}$ is the rotation matrix, representing the direction of the camera coordinate system relative to the global coordinate system. $\boldsymbol{t}$ is the translation vector, namely the translation of camera coordinate system relative to the global coordinate system. $\boldsymbol{C}$ is the coordinates of the camera center in the global coordinate system. [K|0] indicates that the matrix is partitioned into a 3×3 K matrix and a 3×1 column matrix.

The skew parameter $\boldsymbol{s}$ is that a skewing of the pixel elements in the CCD array so that the x-axes and the y-axes are not perpendicular to each other. In realistic circumstances a

$$R(\gamma,\theta,\phi)=\begin{bmatrix} cos\phi cos\gamma+sin\theta sin\phi sin\gamma & cos\theta sin\phi & sin\phi sin\theta cos\gamma-cos\phi sin\gamma \\ cos\phi sin\theta sin\gamma-sin\phi cos\gamma & cos\theta cos\phi & sin\phi sin\gamma+sin\theta cos\phi cos\gamma \\ cos\theta sin\gamma & -sin\theta & cos\theta cos\gamma \end{bmatrix} \tag{3}$$

non-zero skew might arise as a result of taking an image of an image, for example if a photograph is re-photographed, or a negative is enlarged. Therefore, for most standard cameras, the skew parameter**s** is 0. So in this paper, the camera's internal parameter matrix K is composed of four elements, its expression is simplified as follows: $K=\begin{bmatrix} f_x & 0 & u_x \\ 0 & f_y & u_y \\ 0 & 0 & 1 \end{bmatrix}$.

Usually we call $\boldsymbol{K}$ the internal parameter of the camera. $\boldsymbol{K}$ has four degrees of freedom, namely f_x, f_y, u_x, u_y. The parameters of $\boldsymbol{R}$ and $\boldsymbol{C}$ are related to the direction and position of the camera in the global coordinate system. We usually call them external parameters, and $\boldsymbol{R}$ and $\boldsymbol{C}$ each have three degrees of freedom. $\boldsymbol{P}$ is the camera matrix.

B. DEFINITION OF TARGET COORDINATE SYSTEM

The target graph is shown in Fig. 1, the $\boldsymbol{o}$ is the origin of the coordinate system, and the $\boldsymbol{x}$ and $\boldsymbol{y}$ axes are shown in Fig. 1 (a), and the z axis is determined according to the right-handed coordinate system. The target is an equilateral right triangle, and the two right angles edges are L respectively. The target consists of 9 feature points and 9 feature lines.

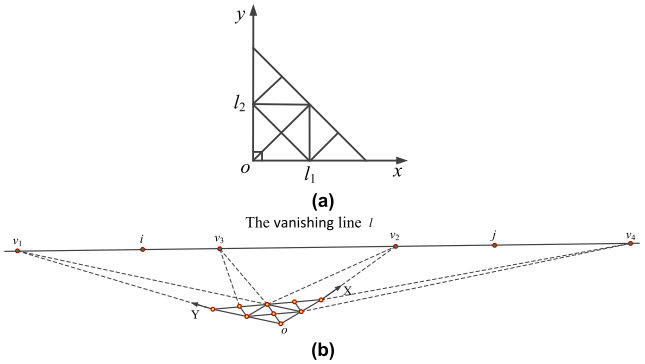

FIGURE 1. The coordinate system of the target and the plane perspective projection. (a) The top view of the target. (b) The perspective projection of the target.

According to the target coordinate system, the Euler angles (Z-X-Y) of the rotation matrix can be defined by yaw angle $\boldsymbol{\gamma}$, pitch angle $\boldsymbol{\theta}$ and roll angle $\boldsymbol{\varphi}$. The transformation relationship is shown in (3), as shown at the top of this page.

Fig. 1 (b) is a perspective projection of a target, where $\boldsymbol{v_1}$, $\boldsymbol{v_2}$, $\boldsymbol{v_3}$, $\boldsymbol{v_4}$ are the vanishing points, $\boldsymbol{i}$ and $\boldsymbol{j}$ are the images of the imaginary dots, and $\boldsymbol{l}$ is the vanishing line.

C. VANISHING POINT AND VANISHING LINE

Geometrically, the vanishing point of a 3-D space line is obtained by the intersection of the ray that is parallel to the line and through the center of the camera and the plane of the image. Therefore, the vanishing point only depends on the direction of the straight line and has nothing to do with its location. The vanishing point is an image of infinity, unaffected by the change in camera position. It is only affected by the rotation of the camera.

Conclusion 1: The vanishing point of the 3-D space line with direction $\boldsymbol{d}$ is the intersection point $\boldsymbol{v}$ of the ray with the direction of $\boldsymbol{d}$ and the plane of the image [11]. It can be expressed as

$$v=Kd \tag{4}$$

The parallel plane of the 3-D space is intersected with the infinite plane π_∞ in a common straight line, and the image of this line is the vanishing line of the plane. The vanishing line is only related to the orientation of the scene plane, not its location. The vanishing line of the plane π is obtained by the intersection of the plane passing through the center $\boldsymbol{C}$ of the camera and the plane of the image.

Conclusion 2: In the camera Euclidean coordinate system, the vanishing line of the plane set perpendicular to the direction $\boldsymbol{n}$ is [11]:

$$l=K^{-T}n \tag{5}$$

D. THE IMAGE OF THE ABSOLUTE QUADRATIC CURVE (IAV)

In the non-homogeneous coordinate system, the equation of the quadratic curve is:

$$ax^2+bxy+cy^2+dx+ey+f=0 \tag{6}$$

In the homogeneous coordinate system, let $x=x_1/x_3$, $y=x_2/x_3$ and the quadratic curve is:

$$ax_1^2+bx_1x_2+cx_2^2+dx_1x_3+ex_2x_3+fx_3^2=0 \tag{7}$$

The form of a matrix is: $x^TCx=0$, where, $C=\begin{bmatrix} a & b/2 & d/2 \\ b/2 & c & e/2 \\ d/2 & e/2 & f \end{bmatrix}$.

The quadratic curve has five degrees of freedom, and its ratio is: $\{a:b:c:d:e:f\}$, equivalent to the number of elements of the symmetric matrix minus one degree of freedom [11].

The absolute quadratic curve Ω_∞ is a quadratic curve on the infinite plane π_∞. In the homogeneous coordinate system $\pi_\infty=(0,0,0,1)^T$, the points on Ω_∞ satisfy the following conditions:

$$\begin{cases} X_1^2+X_2^2+X_3^2=0 \\ X_4^2=0 \end{cases} \tag{8}$$

All circles cross Ω_∞ at two points and these two points are imaginary dots. The imaginary dot is a pair of complex conjugate ideal points, whose standard form is: $I = [1, i, 0]^T$, $J = [1, -i, 0]^T$.

Conclusion 3: The image of absolute quadratic curve (IAC) is a quadratic curve:

$$w = (KK^T)^{-1} = K^{-T}K^{-1} \tag{9}$$

The image of the absolute quadratic curve (IAC) $\boldsymbol{w}$ is only related to the internal parameter $\boldsymbol{K}$ of the camera matrix $\boldsymbol{P}$, which has nothing to do with the orientation and location of the camera. The image of the imaginary dot is the point on $\boldsymbol{w}$, which is the intersection of the vanishing line of the plane π and $\boldsymbol{w}$.

Under orthogonal conditions, the vanishing point, vanishing line and IAC have the following important properties:

(1) The vanishing point of a line with vertical direction is satisfied when $v_1^T w v_2 = 0$

(2) The relationship between the vanishing point $\boldsymbol{v}$ of a plane normal direction and the vanishing line $\boldsymbol{l}$ of the plane is $l = wv$.

E. THE INVARIANCE OF PERSPECTIVE PROJECTION

If $\boldsymbol{A}$,$\boldsymbol{B}$,$\boldsymbol{C}$,$\boldsymbol{D}$ are four points on a single column, their coordinates are $\boldsymbol{a, b, c, d}$, and then the cross ratio of the 4 points $\boldsymbol{A}$, $\boldsymbol{B}$, $\boldsymbol{C}$, $\boldsymbol{D}$ are represented by $\boldsymbol{R(A,B,C,D)}$ or $\boldsymbol{R(a,b,c,d)}$, and the relationship is as follows [12]:

$$R(A, B, C, D) = R(a, b, c, d) = \frac{a-c}{b-c} : \frac{a-d}{b-d} \tag{10}$$

Under the projective transformation of any straight line, the value of the cross ratio is the same, i.e., the intersection ratio is the basic projective invariant.

If the four points, $\boldsymbol{A}$, $\boldsymbol{B}$, $\boldsymbol{C}$, $\boldsymbol{D}$, cross the ratio $R(A, B, C, D) = 1$, these points are called harmonic points, which constitute a harmonic point sequence. According to point $\boldsymbol{C}$ and $\boldsymbol{D}$ harmonic to point $\boldsymbol{A}$ and $\boldsymbol{B}$ (point pair $\boldsymbol{C}$, $\boldsymbol{D}$ harmonic to point pair $\boldsymbol{A}$, $\boldsymbol{B}$), or $\boldsymbol{A}$ and $\boldsymbol{B}$ harmonic to point $\boldsymbol{C}$ and $\boldsymbol{D}$ (point pair $\boldsymbol{A}$, $\boldsymbol{B}$ harmonic to point pair $\boldsymbol{C}$, $\boldsymbol{D}$), also called $\boldsymbol{D}$ for $\boldsymbol{A}$, $\boldsymbol{B}$, $\boldsymbol{C}$ on the fourth harmonic point and $\boldsymbol{A}$, $\boldsymbol{B}$ and $\boldsymbol{C}$, $\boldsymbol{D}$ into harmonic conjugate.

At any point in the plane, the two straight lines lead to the imaginary dot. $\boldsymbol{I}$and $\boldsymbol{J}$ are called the two isotropic straight lines that passing through the point. They are called the isotropic direction along the direction of the isotropic straight line.

Lager's theorem: Assuming that the angle between the two non-isotropic lines is $\boldsymbol{\theta}$, the cross ratio between the two lines and the two isotropic lines with their intersection points at -$\boldsymbol{i}$and $\boldsymbol{i}$ slopes is $\boldsymbol{\mu}$ [12]. There are:

$$\theta = \frac{1}{2i}\ln\mu \quad \text{or } \mu = e^{2i\theta} \tag{11}$$

Corollary: when the two intersections of two straight lines and infinity lines l_∞ are the harmonic conjugation to the imaginary circles $\boldsymbol{I}$ and $\boldsymbol{J}$, then the two lines are perpendicular to each other. That is, $\theta = \pi/2$, $e^{2i\theta} = -1$.

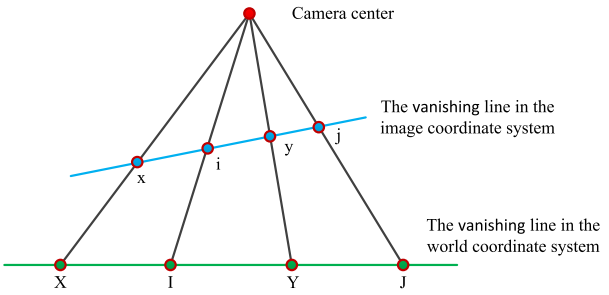

FIGURE 2. Diagram of the invariant characteristics of the intersection ratio.

As shown in Fig. 2, suppose that the two non-isotropic straight lines are perpendicular to each other. According to the inference, the following relations can be obtained:

$$R(X, Y, I, J) = R(x, x, i, j) = -1 \tag{12}$$

F. THE EPIPOLAR GEOMETRY AND THE FUNDAMENTAL MATRIX

Epipolar geometry is the intrinsic projective geometry between the two views. It is independent of the scene structure and depends only on the internal parameters and relative position of the camera. The schematic diagram of the epipolar geometry is shown in Fig. 3. The projection of a single point $\boldsymbol{X}$ on the space plane $\boldsymbol{\pi}$ on the two imaging planes is $\boldsymbol{x}$ and x' respectively. The plane composed of $\boldsymbol{X}$, $\boldsymbol{C}$ and C' is called the epipolar plane, which contains the baseline. The points $\boldsymbol{e}$ and $\boldsymbol{e}'$ are the epipoles. It is the intersection of the straight line between the two camera centers and the image plane, and the epipole is the image of the other camera center in one view. It is also the vanishing point of the baseline direction. $\boldsymbol{l}$ and l' are the epipolar lines, which are the intersection of the epipolar plane and the plane of the image, and all of the epipolar lines are handed to the epipole [11].

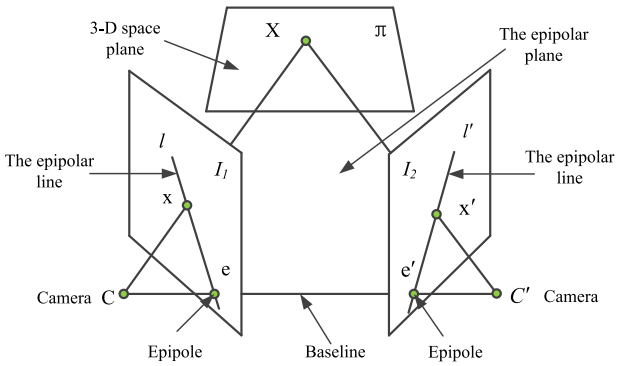

FIGURE 3. Schematic diagram of epipolar geometry.

Conclusion 4: For any pair of corresponding points in two images, the fundamental matrix satisfies the condition: $x'^T F x = 0$.

The fundamental matrix is an algebraic representation of the epipolar geometry. The fundamental matrix has two important properties given as follows:

1) Using the fundamental matrix to find the epipoles: $Fe = 0, F^T e' = 0$.
2) Using the fundamental matrix to find the epipolar lines: $l' = Fx, l = F^T x'$.

III. CAMERA CALIBRATION

The main steps of the calibration method used in this paper are as follows:

a. Adopt the Harris corner point detection algorithm to extract feature points;

b. Use the intersection point of parallel lines or use Lager's theorem and deduction to calculate the vanishing points and use normalized homographic method to get the image of the imaginary dot.

c. The radial distortion and tangential distortion of the camera are obtained by using the cross ratio invariance, and the calibrated target image is de-distorted by using the distortion coefficient.

d. According to the known conditions, calculate the image of the absolute quadratic curve (IAC) $\boldsymbol{w}$ and find the internal parameter matrix $\boldsymbol{K}$.

e. Use the orthogonal property to calculate the rotation matrix $\boldsymbol{R}$, using the center $\boldsymbol{C}$ of the camera to calculate the translation vector $\boldsymbol{t}$;

f. Calculate the Euler angle of the camera by using the vanishing line calculated by the perspective projection model and the vanishing line drawn by the vanishing point fitting.

g. Use the normalized 8-point algorithm to solve the fundamental matrix $\boldsymbol{F}$, and then determine the constraint relationship between different views.

A. FEATURE EXTRACTION

The basic idea of Harris corner detection algorithm is to use a fixed window to slide in any direction on the image, compare the degree of change of the pixel gray level in the fixed window before and after sliding. If there is a large gray scale change in any direction, then we can assume that there are corner points in the window [27], [28].

Harris point detection operator has the following properties: (a) It is insensitive to changes in brightness and contrast; (b) It has rotational invariance; (c) It is not scale invariant.

It is appropriate to use the Harris corner detection algorithm for this target model. The feature points of the target are determined by the intersection points of different straight lines. The gray level changes obviously at the intersection points and the contrast is relatively high. So it is convenient and fast to detect and extract the corner points.

After the Harris corner detection is completed, the corresponding feature points can be obtained, and the corresponding characteristic lines can be fitted by the least square method through the feature points.

B. THE CALCULATION OF THE VANISHING POINT AND THE IMAGE OF THE IMAGINARY DOT

1) THE CALCULATION OF THE VANISHING POINT

A set of parallel lines in 3-D space is intersected to one point in the image plane, which is the vanishing point, i.e., the image of infinity points in the image plane. According to Fig. 1 (b), we can use the intersection point of the image of parallel lines to find four vanishing points, $\boldsymbol{v_1}, \boldsymbol{v_2}, \boldsymbol{v_3}, \boldsymbol{v_4}$ respectively.

Another way to solve the problem is to use Lager's theorem and deduction to obtain the following formula [12], [23].

$$\begin{cases} R(v_1, v_2, i, j) = -1 \\ R(v_3, v_4, i, j) = -1 \\ R(v_2, v_3, i, j) = e^{2i(\pi/4)} \\ R(v_1, v_4, i, j) = e^{2i(3\pi/4)} \end{cases} \tag{13}$$

The vanishing point can be obtained by solving the above equation. The above two methods can be used synthetically, and better results may be obtained.

After finding out four vanishing points, using the least square method to fit four vanishing points, the vanishing line of the image plane can be obtained.

2) A NORMALIZED SINGLE HOMOGRAPHIC METHOD FOR THE IMAGE OF A VIRTUAL CIRCULAR POINT

The normalization of data can not only improve the accuracy of the results, but also eliminate the influence of coordinate transformation by selecting an effective standard coordinate system for the measurement data. The normalization method consists of the following steps [11]:

(1) Shift the coordinates of each image to make the centroid of the point set at the origin;

(2) Scale the point set, so that the average distance between them and the origin is equal to $\sqrt{2}$;

(3) The above transformation is performed independently of two images.

The homography is a mapping transformation from one plane to another, and the homographic matrix is a 3×3 transformation matrix $\boldsymbol{H}$. The homographic transformation is given by the following equation:$x' = Hx$. Using direct linear transformation (DLT) method to solve $\boldsymbol{H}$, because of the same direction, in order to eliminate the influence of non-zero factors, vector cross multiplication is used to indicate that: $x' \times Hx = 0$. Assuming $x_i' = (x_i', y_i', 1)^T$, $x_i = (x_i, y_i, 1)^T$, a pair of homographic points should be able to obtain the following relation:

$$\begin{bmatrix} 0 & -x_i^T & y_i' x_i^T \\ x_i^T & 0 & -x_i' x_i^T \\ -y_i' x_i^T & x_i' x_i^T & 0 \end{bmatrix} h = 0 \tag{14}$$

In order to solve homographic matrix $\boldsymbol{H}$, there are at least 4 sets of corresponding points. In order to improve the accuracy, we can first normalize each image, then solve it with the DLT method, and finally decompose the normalization.

The target is a square in this paper, and the correspondence between its four corner points and their images determines a homography $\boldsymbol{H}$ between the plane of the square π and the image. Usually in order to facilitate calculation, we take the four corners of a square as: $(0,0,1)^{\mathrm{T}}$, $(1,0,1)^{\mathrm{T}}$, $(0,1,1)^{\mathrm{T}}$, $(1,1,1)^{\mathrm{T}}$. If the homography $\boldsymbol{H}$ is applied to the imaginary dot on the plane π, we can get the image of the imaginary dot: $H(1, \pm i, 0)^T$.

C. THE SOLUTION OF DISTORTION PARAMETERS

1) THE INTRODUCTION OF RADIAL AND TANGENTIAL DISTORTION

Distortion is usually characterized by: the principal axis image points are usually taken as the distortion center, because the distortion is symmetrical with respect to the principal axis of the camera lens. The distortion in the center area is the least serious, and the closer it gets to the edge, the more serious the distortion is. The straight line that passes through the principal axis image point is still a straight line after distortion, while other straight lines bend at the edge of the image. For wide-angle cameras, the distortion is relatively more serious. The main purpose of distortion correction is to correct the image measurement approximately to the degree obtained by ideal linear camera and improve the accuracy of image processing. For computer vision, distortion is usually divided into two categories: radial distortion and tangential distortion.

The distortion caused by lens shape is called radial distortion. Radial distortion can be divided into barrel distortion and pincushion distortion. Pincushion distortion is due to the increase of image magnification with the increase of the distance from the optical axis, while barrel distortion is the opposite. Radial distortion can be expressed by a polynomial in terms of coordinate changes before and after distortion.

$$\begin{cases} x_u - e_x = (x_d - e_x)(1 + k_1 r_d^2 + k_2 r_d^4) \\ y_u - e_y = (y_d - e_y)(1 + k_1 r_d^2 + k_2 r_d^4) \end{cases} \tag{15}$$

where, (x_u, y_u) is the pixel coordinate of the ideal point, (x_d, y_d) is the pixel coordinate of the normalized plane point, (e_x, e_y) is the pixel coordinate of the distortion center point, $r_d = \sqrt{(x_d - e_x)^2 + (y_d - e_y)^2}$ is the distance from the distorted image point to the distorted center point, k_1 and k_2 are radial distortion coefficients, wherein, k_1 mainly acts on the image center area with less serious distortion, while k_2 mainly acts on the image edge area with larger distortion.

In the process of assembling camera, the distortion caused by failing to make the lens and imaging plane strictly parallel is called tangential distortion. The tangential distortion is expressed by polynomials as follows:

$$\begin{cases} x_u - e_x = (x_d - e_x) + 2p_1(x_d - e_x)(y_d - e_y) \\ \qquad\qquad + p_2(r_d^2 + 2(x_d - e_x)^2) \\ y_u - e_y = (y_d - e_y) + p_1(r_d^2 + 2(y_d - e_y)^2) \\ \qquad\qquad + 2p_2(x_d - e_x)(y_d - e_y) \end{cases} \tag{16}$$

where, p_1 and p_2 are tangential distortion coefficients.

Let $\bar{x}_u = x_u - e_x, \bar{y}_u = y_u - e_y, \bar{x}_d = x_d - e_x, \bar{y}_d = y_d - e_y$, through the above four distortion coefficients, the correct position of the image point in the pixel coordinate system can be obtained. The formula is as follows:

$$\begin{cases} \bar{x}_u = \bar{x}_d(1 + k_1 r_d^2 + k_2 r_d^4) + 2p_1 \bar{x}_d \bar{y}_d + p_2(r_d^2 + 2\bar{x}_d^2) \\ \bar{y}_u = \bar{y}_d(1 + k_1 r_d^2 + k_2 r_d^4) + p_1(r_d^2 + 2\bar{y}_d^2) + 2p_2 \bar{x}_d \bar{y}_d \end{cases} \tag{17}$$

For most cameras, radial distortion and tangential distortion can be corrected to the extent that the requirements of application are met.

2) THE INTRODUCTION OF DISTORTION CORRECTION METHORDS

In Fig. 4, a_1, b_1, c_1, d_1 and a_2, b_2, c_2, d_2 are the images of A_1, B_1, C_1, D_1 and A_2, B_2, C_2, D_2 in the global coordinate system, respectively. Where D_1 and D_2 are the infinity points in the global coordinate system and d_1 and d_2 are the corresponding vanishing points. Suppose that A_1, B_1, C_1, D_1 and A_2, B_2, C_2, D_2 are in a line, respectively. According to the cross ratio theorem, we can get that:

$$R(A_1, B_1, C_1, D_1) = R(a_1, b_1, c_1, d_1) = \frac{A_1C_1/B_1C_1}{A_1D_1/B_1D_1} \tag{18}$$

where, A_1C_1, B_1C_1, A_1D_1 and B_1D_1 respectively correspond to the distance between two points in the global coordinate system. Since D_1 is the infinity point, namely $A_1D_1/B_1D_1 \approx 1$, the above equation can be simplified as:

$$R(a_1, b_1, c_1, d_1) = A_1C_1/B_1C_1 \tag{19}$$

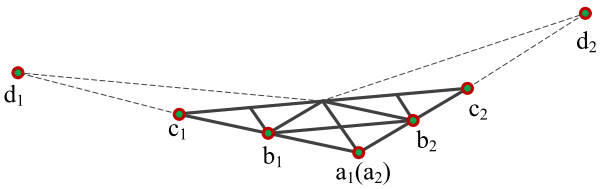

FIGURE 4. A schematic diagram of distortion correction using cross-ratio invariance.

Suppose that in the image coordinate system, the coordinates of four ideal points are $a_1(x_1, y_1)$, $b_1(x_2, y_2)$, $c_1(x_3, y_3)$, $d_1(x_4, y_4)$. Because a_1 and b_1 are relatively close to the center, the distortion is relatively less serious, and the projection of d_1 at infinity is also relatively less serious, so we assume that the coordinates of a_1, b_1, d_1 and ideal point are the same. Because c_1 is at the edge of the image, affected by the distortion, the coordinates of the ideal point deviate from those of the actual image point. According to a_1, b_1 and d_1, the position of ideal point c_1 can be obtained. According to (19), we can get the coordinates of c_1 as follows:

$$\begin{cases} x_3 = \dfrac{R \cdot x_2(x_1 - x_4) - x_1(x_2 - x_4)}{R \cdot (x_1 - x_4) - (x_2 - x_4)} \\ y_3 = \dfrac{R \cdot y_2(y_1 - y_4) - y_1(y_2 - y_4)}{R \cdot (y_1 - y_4) - (y_2 - y_4)} \end{cases} \tag{20}$$

Similarly, we can obtain the coordinates of ideal and actual points of a_2, b_2, c_2 and d_2.

According to (17), we can obtain four equations of distortion parameters:

$$\begin{bmatrix} \bar{x}_{d1}r_{d1}^2 & \bar{x}_{d1}r_{d1}^4 & 2\bar{x}_{d1}\bar{y}_{d1} & r_{d1}^2+2\bar{x}_{d1}^2 \\ \bar{y}_{d1}r_{d1}^2 & \bar{y}_{d1}r_{d1}^4 & r_{d1}^2+2\bar{y}_{d1}^2 & 2\bar{x}_{d1}\bar{y}_{d1} \\ \bar{x}_{d2}r_{d2}^2 & \bar{x}_{d2}r_{d2}^4 & 2\bar{x}_{d2}\bar{y}_{d2} & r_{d2}^2+2\bar{x}_{d2}^2 \\ \bar{y}_{d2}r_{d2}^2 & \bar{y}_{d2}r_{d2}^4 & r_{d2}^2+2\bar{y}_{d2}^2 & 2\bar{x}_{d2}\bar{y}_{d2} \end{bmatrix} \cdot \begin{bmatrix} k_1 \\ k_2 \\ p_1 \\ p_2 \end{bmatrix} = \begin{bmatrix} \bar{x}_{u1}-\bar{x}_{d1} \\ \bar{y}_{u1}-\bar{y}_{d1} \\ \bar{x}_{u2}-\bar{x}_{d2} \\ \bar{y}_{u2}-\bar{y}_{d2} \end{bmatrix} \quad (21)$$

Formula (21) can be written in the form of a matrix:

$$M \cdot q = m \quad (22)$$

where $\boldsymbol{q}$ is a distorted parameter matrix, $q = \begin{bmatrix} k_1 & k_2 & p_1 & p_2 \end{bmatrix}^T$.

Using the linear least squares method, the value of the distortion parameter matrix $\boldsymbol{q}$ can be obtained as follows:

$$q = (M^T \cdot M)^{-1} M^T \cdot m \quad (23)$$

Thus, the initial estimation of the distortion parameter matrix $\boldsymbol{q}$ is obtained. In order to reduce the error and improve the accuracy of the distortion parameter, LM algorithm is used for the nonlinear optimization of the error function below. The optimization function is as follows:

$$Q = \sum_{i=1}^{n} [(\bar{x}_u^i - \tilde{x}_u^i)^2 + (\bar{y}_u^i - \tilde{y}_u^i)^2] \quad (24)$$

where, $\bar{x}_u^i$ and $\bar{y}_u^i$ are pixel coordinates after correction of distortion obtained according to (17); $\tilde{x}_u^i$ and $\tilde{y}_u^i$ are ideal pixel coordinates without distortion; and n is the number of distorted images.

So far, the parameters of radial and tangential distortion can be obtained.

D. CALCULATE THE IAC W AND FIND OUT THE INNER PARAMETER MATRIX K

According to the expression of the inner parameter matrix $\boldsymbol{K}$, we can get the expression of $\boldsymbol{w}$ as follows:

$$w = (KK^T)^{-1} = \frac{1}{f_x^2 f_y^2} \begin{bmatrix} f_y^2 & 0 & -f_y^2 u_x \\ 0 & f_x^2 & -f_x^2 u_y \\ -f_y^2 u_x & -f_x^2 u_y & f_x^2 f_y^2 + u_x^2 f_x^2 + u_y^2 f_y^2 \end{bmatrix} \quad (25)$$

According to the method provided in the Section ć6.B, we can find the image of the virtual dot as: $i = H(1, i, 0)^T, j = H(1, -i, 0)^T$. Because both $\boldsymbol{i}$ and $\boldsymbol{j}$ are on IAC, they meet the following:

$$\begin{cases} i^T w i = 0 \\ j^T w j = 0 \end{cases} \quad (26)$$

In Fig. 1, $\boldsymbol{l_1}$ and $\boldsymbol{l_2}$ are perpendicular to each other. According to the inference of Lager's theorem, we can get the vanishing points in the straight line of $\boldsymbol{l_1}$ and $\boldsymbol{l_2}$ to satisfy the following relations:

$$v_1^T w v_2 = 0 \quad (27)$$

The same reason can be obtained:

$$v_3^T w v_4 = 0 \quad (28)$$

According to (26) (27) (28), the value of $\boldsymbol{w}$ can be solved. Assuming $w = \begin{bmatrix} w_{11} & 0 & w_{13} \\ 0 & w_{22} & w_{23} \\ w_{13} & w_{23} & w_{33} \end{bmatrix}$, the inner parameter matrix $\boldsymbol{K}$ can be obtained according to the relational formula (25), as shown below:

$$\begin{cases} f_x^2 = \dfrac{\det(w)}{w_{11}^2 w_{22}} \\ f_y^2 = \dfrac{\det(w)}{w_{11} w_{22}^2} \\ u_x = -\dfrac{w_{13}}{w_{11}} \\ u_y = -\dfrac{w_{23}}{w_{22}} \\ \det(w) = w_{11}w_{22}w_{33} - w_{11}w_{23}^2 - w_{22}w_{13}^2 \end{cases} \quad (29)$$

Another way to solve for $\boldsymbol{K}$ is to first obtain the inverse matrix of $\boldsymbol{w}$ and then use the Cholesky decomposition to get the value of $\boldsymbol{K}$.

E. THE CALCULATION OF THE ROTATION MATRIX R AND THE TRANSLATION VECTOR t

1) THE CALCULATION OF THE ROTATION MATRIX R

According to Fig. 1, $\boldsymbol{v_1}$ is the vanishing point in the $\boldsymbol{Y}$ axis and $\boldsymbol{v_2}$ is the vanishing point in the $\boldsymbol{X}$ axis. According to the formula $d = K^{-1}v$, the direction vector of the $\boldsymbol{X}$ axis can be obtained as follows: $d_x = K^{-1}v_2$; the direction vector of the $\boldsymbol{Y}$ axis is $d_y = K^{-1}v_1$. According to the orthogonality of the rotation matrix, we can get the rotation matrix of the camera coordinate system relative to the global coordinate system.

$$R = \begin{bmatrix} \frac{d_x}{\|d_x\|} & \frac{d_y}{\|d_y\|} & \frac{d_x \times d_y}{\|d_x \times d_y\|} \end{bmatrix} \quad (30)$$

2) THE CALCULATION OF THE TRANSLATION VECTOR T

Assuming that the direction of the $\boldsymbol{Z}$ axis in the 3-D space is $d_z = d_x \times d_y$, then according to the formula $v_z = Kd_z$, we can find out the vanishing points in the $\boldsymbol{Z}$ axis. Using the three vertical direction vanishing points in$\boldsymbol{X}$ axis, the $\boldsymbol{Y}$ axis and the $\boldsymbol{Z}$ axis, the vertical center of the triangle formed by these three points is the center $\boldsymbol{C}$ of the camera.

Assume that $\boldsymbol{v_x} = (x_1, y_1, z_1)$, $\boldsymbol{v_y} = (x_2, y_2, z_2)$, $\boldsymbol{v_z} = (x_3, y_3, z_3)$, C = (x, y, z). According to Kramer's law, the following formula can be obtained:

$$\begin{aligned} a &= x_1(x_3 - x_2) + y_1(y_3 - y_2) + z_1(z_3 - z_2) \\ b &= x_2(x_3 - x_1) + y_2(y_3 - y_1) + z_2(z_3 - z_1) \\ c &= x_3(x_2 - x_1) + y_3(y_2 - y_1) + z_3(z_2 - z_1) \end{aligned}$$

$$
\begin{aligned}
D &= \det\begin{pmatrix} x_3-x_2 & y_3-y_2 & z_3-z_2 \\ x_3-x_1 & y_3-y_1 & z_3-z_1 \\ x_2-x_1 & y_2-y_1 & z_2-z_1 \end{pmatrix}, \\
D_x &= \det\begin{pmatrix} a & y_3-y_2 & z_3-z_2 \\ b & y_3-y_1 & z_3-z_1 \\ c & y_2-y_1 & z_2-z_1 \end{pmatrix} \\
D_y &= \det\begin{pmatrix} x_3-x_2 & a & z_3-z_2 \\ x_3-x_1 & b & z_3-z_1 \\ x_2-x_1 & c & z_2-z_1 \end{pmatrix}, \\
D_z &= \det\begin{pmatrix} x_3-x_2 & y_3-y_2 & a \\ x_3-x_1 & y_3-y_1 & b \\ x_2-x_1 & y_2-y_1 & c \end{pmatrix} \\
x &= \frac{D_x}{D}, \quad y = \frac{D_y}{D}, \; z = \frac{D_z}{D}
\end{aligned} \tag{31}
$$

The coordinates of $\boldsymbol{C}$ obtained above are the location of the camera center in the global coordinate system. Using the formula $t = -RC$, the translation vector can be obtained.

The internal and external parameters of the camera are now figured out.

F. FINDING THE EULER ANGLE OF THE CAMERA

If the $\boldsymbol{X}$ axis is used as the benchmark, assuming that the direction vector of the $\boldsymbol{X}$ axis is $d_x = (x_1, x_2, x_3)$, then the yaw angle is:

$$
\gamma = \arccos\left(\frac{x_1}{\sqrt{x_1^2 + x_2^2}}\right) \tag{32}
$$

Using the method outlined in Section ćó.B, the equation of the vanishing line can be obtained as follows:

$$
au + bv + c = 0 \tag{33}
$$

It is assumed that in the 3-D space, the infinity point is $\tilde{X}_i = [x_i, y_i, 0, 0]^T$. According to the perspective projection model:

$$
\begin{aligned}
s\tilde{x}_i &= K[R|t]\tilde{X}_i (i = 1, 2) \\
K &= \begin{bmatrix} f_x & 0 & u_x \\ 0 & f_y & u_y \\ 0 & 0 & 1 \end{bmatrix}, \quad R = \begin{bmatrix} R_{11} & R_{12} & R_{13} \\ R_{21} & R_{22} & R_{23} \\ R_{31} & R_{32} & R_{33} \end{bmatrix}, \\
t &= \begin{bmatrix} t_1 & t_2 & t_3 \end{bmatrix}^T
\end{aligned} \tag{34}
$$

Therefore, the vanishing points obtained from the infinite point projection are:

$$
\tilde{x}_i = \begin{bmatrix} f_x \dfrac{R_{11}x_i + R_{12}y_i}{R_{31}x_i + R_{32}y_i} + u_x & f_y \dfrac{R_{21}x_i + R_{22}y_i}{R_{31}x_i + R_{32}y_i} + u_y & 1 \end{bmatrix}^T \tag{35}
$$

The vanishing line can be obtained according to $l = \tilde{x}_1 \times \tilde{x}_2$. The direction is given in (36), as shown at the bottom of this page.

Using equation (34) to further simplify, the equation of the vanishing line can be obtained as follows:

$$
-\frac{sin\phi}{f_x}u + \frac{tan\theta}{f_y}v + \frac{sin\phi}{f_x}u_x - \frac{tan\theta}{f_y}u_y + cos\phi = 0 \tag{37}
$$

Comparison of equations (33) and (37) can be used to calculate the pitch angle θ and the roll angle φ, and the expression is as follows:

$$
\begin{cases} \phi = arctan\left(\dfrac{-af_x}{au_x + bu_y + c}\right) \\ \theta = arctan\left(-\dfrac{b}{a}\dfrac{f_y}{f_x}sin\phi\right) \end{cases} \tag{38}
$$

According to the above method, the azimuth angle of the camera relative to the global coordinate system can be obtained.

G. NONLINEAR OPTIMIZATION

The above calibration results are the camera's internal and external parameters and azimuth angle. Although the camera model can well express a camera, the calibration results will be erroneous because the data will be influenced by various noises. Therefore, nonlinear optimization method is needed to reduce the effect of noise on calibration results.

The above calibration results are taken as the initial value of optimization. The image pixel coordinates obtained by the reprojection are subtracted from the original image pixel coordinates to minimize the error and to obtain the optimal value of camera internal and external parameters.

$$
L = min\sum_{i=1}^{N}\left\|\tilde{x}_i - K[R|t]\tilde{X}_i\right\|^2 \tag{39}
$$

where, $\tilde{x}_i$ is the pixel coordinates of the i feature points of the original image, $\tilde{X}_i$ is the coordinates of the i characteristic point in the global coordinate system, N is the total number of feature points.

The optimal solution of the camera's internal and external parameters can be obtained through the LM method.

H. SOLVING THE FUNDAMENTAL MATRIX F

When using the sequence image to calibrate, we need to calculate the fundamental matrix $\boldsymbol{F}$, so that the relative relation between the sequence images can be obtained. The fundamental matrix $\boldsymbol{F}$ is usually obtained by the normalized eight-point algorithm [30].

The normalized eight-point algorithm includes the following four steps: normalization, solving linear solutions,

$$
l = \begin{bmatrix} f_y(R_{21}R_{32} - R_{22}R_{31}) \\ f_x(R_{12}R_{31} - R_{11}R_{32}) \\ f_xf_y(R_{11}R_{22} - R_{12}R_{21}) + u_xf_y(R_{22}R_{31} - R_{32}R_{21}) + u_yf_x(R_{11}R_{32} - R_{31}R_{12}) \end{bmatrix} \tag{36}
$$

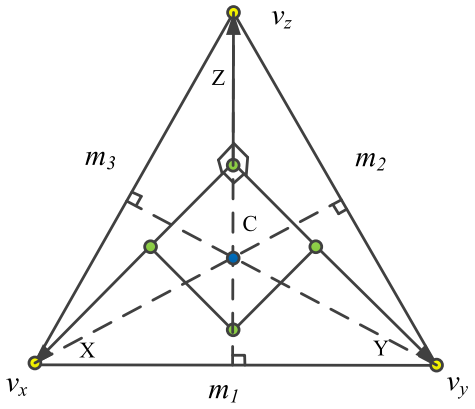

FIGURE 5. Solve the vertical center of the triangle with the vanishing point as the vertex.

forcing constraints and de-normalization. The value obtained is regarded as the initial value, and then the LM method is used to optimize it, and the optimal solution F is obtained.

$$\tilde{F} = \sum_{i=1}^{n} (x_i - Fx_i')^2 \tag{40}$$

where, x_i and x' are the matching point pairs in the two images, and n is the number of matching point pairs.

According to the formula $Fe = 0, F^T e' = 0$, the epipoles of the epipolar geometry can be obtained, which is the image of the camera in the other view and also the vanishing point of the base line. According to the formula $l' = Fx, l = F^T x'$, we can find out the epipolar line in two images in view of a point in space.

Fig. 6 shows the projection of all camera centers and their epipolar geometry relationships after circular motion of the camera around the target [21], [23]. In the instance C_1, C_2 and C_i are the centers of the camera in the global coordinate system, all camera centers are in a plane. The rotation angle of the camera from C_1 to C_2 is $\boldsymbol{\theta}$, the circumference angle $\angle C_1 C_i C_2$ is φ, the relationship between $\boldsymbol{\theta}$ and φ is $\theta = 2 * \phi$. The $\boldsymbol{e_{i1}}$ and $\boldsymbol{e_{i2}}$ are the projections of camera center C_1 and C_2 in camera C_i, which are the epipoles. $\boldsymbol{i}$ and $\boldsymbol{j}$ are the images of the imaginary dots in the image plane of the camera C_i, respectively.

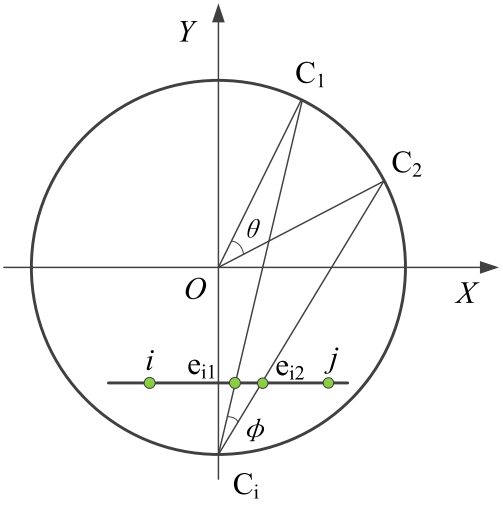

FIGURE 6. The projection of the center of the camera and the epipolar geometric relation.

According to the Lager's theorem, we can get the following:

$$\phi = \frac{1}{2i} ln(R(e_{i1}, e_{i2}, i, j)) \tag{41}$$

The rotation angle of the two cameras can be obtained using the formula $\theta = 2 * \phi$.

IV. ANALYSIS OF EXPERIMENTAL RESULTS

The physical experiment used in this paper is shown in Fig. 7. A GoPro HERO 6 digital camera is fixed to a tripod and the target is taken by adjusting the position of the camera by adjusting the tripod or control rod. The resolution of the digital camera is: 4000 pixels × 3000 pixels. The Gopro has four visual field modes: wide, linear, medium and narrow.

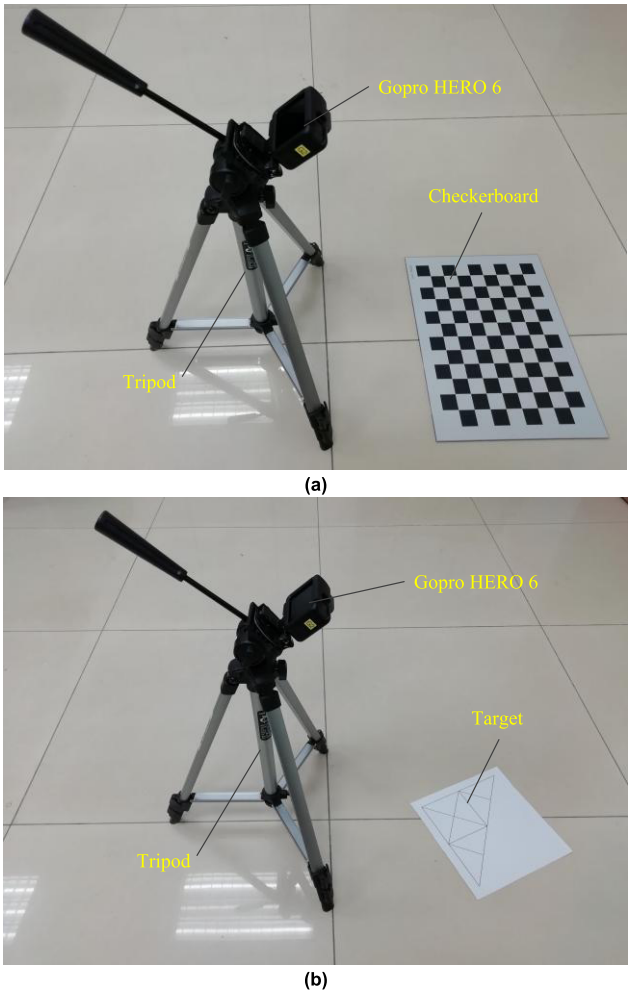

FIGURE 7. Picture of the physical experiment. (a) Calibrate the camera with a checkerboard. (b) Calibrate the camera with the target.

We choose the linear field of view mode to minimize the distortion.

A. CAMERA DE-DISTORTION EXPERIMENT

The radial and tangential distortion parameters of the camera can be obtained by using the method proposed in this paper. The results are shown in Table 1.

TABLE 1. The solution of distortion coefficient.

Parameter	k_1	k_2	p_1	p_2
Result	3.881e-08	-8.105e-15	5.802e-07	3.407e-06

The target image is de-distorted by using the distortion coefficient, and the images before and after the processing are shown in the Fig. 8 (a) (b), respectively.

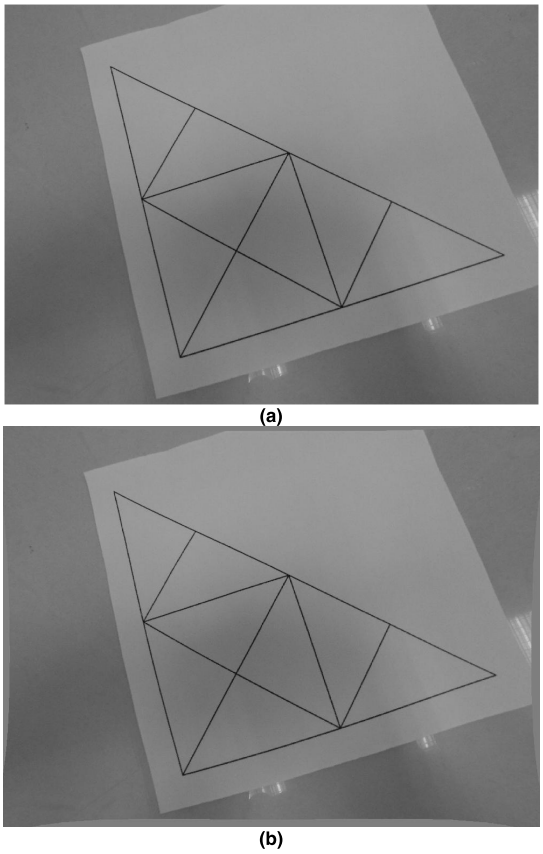

FIGURE 8. Comparison of target image before and after correction. (a) Before correction. (b) After correction.

By comparing the images, we can find that the distortion of the target image is relatively less serious, and the difference between the results before and after correction is not very significant, which shows that the camera has a good linearity and almost no distortion to the image.

B. COMPARISON OF CALIBRATION RESULTS OF CAMERA INTERNAL PARAMETERS

In this paper, we used a checkerboard to calibrate the camera internal parameters, and the result acts as the benchmark for comparison. The tool used was Bouguet camera calibration toolbox in Matlab [31]. The space between the checkerboard cells used was 25mm. In order to improve the accuracy of the parameters in the target calibration camera and reduce the influence of random factors on the calibration results, the following measures were adopted: First, the tripod was placed in different positions and at different angles to take a number of group photographs. It was ensured that the size of the target image accounted for 1/3 $\sim$ 3/4 of the entire image size, and it was distributed at different positions of the image. Second, the photo in each group was calibrated several times, the average value calculated, and then the average of the calibration results of all groups was measured again to minimize the influence of random factors as much as possible. Third, all experimental data were normalized to minimize the error caused by coordinate transformation. The calibration results of camera internal parameters are shown in the following table.

TABLE 2. Alibration results of camera internal parameters.

		f_x	f_y	u_x	u_y
Checkerboard		2084.5	2040.7	2003.0	1415.4
Distortion	Target	2114.5	1977.0	2176.8	1372.8
	Error	1.44%	3.12%	8.68%	3.01%
De-distortion	Target	2120.4	1984.9	2153.8	1364.4
	Error	1.72%	2.74%	7.53%	3.60%

It can be seen from the calibration results that the calibration results of distorted target and de-distorted target are not too different from the checkerboard calibration results, indicating that the distortion caused by camera has little impact on the calibration of the target. It can be seen from the calibration results that the error in some parameters is large, and the possible reasons are as follows: in the calibration process, human factors may have influenced the calibration results. Since filtering is not used in the calibration process, some image noises may have an effect on the result. The amount of calibration data used is not enough, which may influence the precision. However, the error in most calibration results is controlled within 5%, so the calibration results can be used and can meet the precision requirements of most commonly used environments.

C. THE INFLUENCE OF YAW ANGLE AND PITCH ANGLE ON CALIBRATION RESULTS

Since different yaw angles and pitch angles will affect the calibration results, the following research will be studied on the influence of yawing angles and pitching angles. The true values of yaw and pitch angles are obtained by repeated measurements and adjustments with protractors.

1) THE INFLUENCE OF YAW ANGLE ON CALIBRATION RESULTS

Since the target is positioned relative to the camera, in the study of the influence of the yaw angle on the calibration

results, the position and attitude of the camera can be kept constant. The target is rotated at its center, and it is placed in the middle of the image as much as possible. The rotation angle is the yaw angle of the camera. The results of the experiment are shown in the following table.

TABLE 3. The influence of the yaw angle on the calibration results.

		f_x	f_y	u_x	u_y
Checkerboard		2084.5	2040.7	2003.0	1415.4
0°	Result	2010.9	1509.1	1976.5	787.1
	Error	3.53%	26.05%	1.32%	44.39%
30°	Result	2220.7	1953.0	2061.3	1264.7
	Error	6.53%	4.30%	2.91%	10.65%
45°	Result	2098.4	1778.9	2133.4	971.6
	Error	0.67%	12.83%	6.51%	31.36%
60°	Result	2167.6	2088.1	1994.4	1209.0
	Error	3.99%	2.32%	0.43%	14.58%
90°	Result	2642.3	2080.9	1949.6	460.2
	Error	26.76%	1.97%	2.67%	67.49%

The calibration results obtained at yaw angles 0° and 90° are the worst, followed by the results of yaw angle 45°. The calibration results of 30° and 60° are better. This is because when the yaw angle is either 0° or 90°, the line between the center of the camera and the space origin is perpendicular to the target coordinate axis or characteristic line. At this time, the vanishing point in the vertical line direction is infinitely far away, which generates a large error compared with the position of the vanishing point in other characteristic line directions. This will affect the final calibration result, so the calibration result is the worst. When the yaw angle is 45°, the connection line between the center of the camera and the space origin is parallel to the target feature line. The position of the vanishing point in the direction of this straight line and that of other characteristic lines will also produce a large error, but smaller than the vertical influence. Hence the calibration result is better than that of 0° and 90°. Only when the line, which is between the center of the camera and the space origin, and the characteristic lines in the target are neither vertical nor parallel, the results of the calibration will be ideal, so the results of the yaw angles 30° and 60° are better.

2) THE INFLUENCE OF PITCH ANGLE ON CALIBRATION RESULTS

When the position of the target and camera is fixed, the pitch angle mainly affects the position of the target in the image. The experimental results are shown in the table below.

The experimental results show that when the pitch angle is −30° and −60°, the calibration results are relatively poor, and the calibration results are good when the pitch angle is −45°. This is mainly because when the pitch angle is −30° and −60° in the experiment, the target is relatively close to the edge of the image, and it is easy for image distortion to occur at the edges, which will affect the final calibration result. When the pitch angle is −45°, the target is right in the middle of the image, and its distortion is relatively less serious, so the calibration results are relatively accurate.

TABLE 4. The influence of the pitch angle on the calibration results.

		f_x	f_y	u_x	u_y
Checkerboard		2084.5	2040.7	2003.0	1415.4
-30°	Result	1673.5	1306.5	2035.3	1681.4
	Error	19.72%	35.98%	1.61%	18.79%
-45°	Result	2083.7	1856.3	2045.4	1261.1
	Error	0.04%	9.04%	2.12%	10.90%
-60°	Result	1792.3	1485.2	2124.3	1237.1
	Error	14.02%	27.22%	6.06%	12.60%

There is one point to be explained here. In this paper, the pitch angle of −45° is better due to the height of the tripod and the size of the target, but it is not recommended to use the pitch angle of −45° for all camera calibration. Depending on the circumstances, the pitch angle is most appropriate as long as the target is in the middle of the image.

D. CALCULATE THE ROTATION ANGLE BETWEEN IMAGE SEQUENCES USING THE FUNDAMENTAL MATRIX

In this experiment, the posture and position of the camera remain unchanged, and the target rotates around the origin, which is equivalent to the rotation of the camera around the target. Sequential images are acquired by shooting the target in turn. The fundamental matrix between different sequence images is calculated, and then the epipoles are obtained. Finally, the rotation angle of the target is calculated by using equation (41). The basic principle of calculating the rotation angle by using the fundamental matrix is shown in Fig. 6. In the contrast experiment, the rotation angle of the target is calculated by the difference of the yaw angle of the different positions of the camera. The results of the experiment are shown in the following table.

TABLE 5. Comparison of rotation angles calculated by fundamental matrix and yaw angle.

Standard value		15°	30°	45°	60°
Yaw angle	Result	15.99°	32.80°	48.21°	65.32°
	Error	6.60%	9.33%	7.13%	8.87%
Fundamental matrix	Result	14.41°	30.95°	44.72°	61.15°
	Error	3.93%	3.17%	0.62%	1.92%

It can be seen from the comparison results that the rotation angle calculated by the fundamental matrix is more accurate than that calculated by the yawing angle. The reasons for the poor accuracy of calculating the rotation angle using the yawing angle are as follows: First, the roll angle and pitch

angle will have a certain influence on the calculation of the yaw angle. This is especially true for the roll angle, since the coupling phenomenon of the roll angle and the yaw angle is more serious, and the roll angle will affect the calculation precision of the yaw angle. Second, the artificial operation error will also have certain influence on the result. Third, the calibration results of camera parameters will directly affect the calculation accuracy of yaw angle. The fundamental matrix reflects the position relationship between two images, which is a point to point homography relationship. It is not affected by the roll angle and the calibration results of camera parameters, so the calculation results are relatively accurate.

E. DISCUSSIONS

Through the experiment, we can conclude that: for the calibration result of the camera, the effect of image distortion on the final calibration result is inapparent, and the linear performance of the image is better. When the target is calibrated, the connection of the center of the camera and the target space origin should be avoided in parallel or perpendicular to the target coordinate axis or the characteristic line. The angle selection of the pitch angle and the yaw angle has no fixed range. It should be determined according to the actual situation as much as possible to ensure the target is in the middle of the image, and accounts for about 1/3 of the whole picture. So for this case, the yaw angle is 30° or 60°, and the pitch angle is −45°. It is more accurate to calculate the rotation angle of the camera using the fundamental matrix than to calculate the rotation angle using the yawing angle.

V. CONCLUSION

In this paper, a new calibration target is designed for the calibration of internal and external parameters of the camera. By calculating the target image, the solution of image distortion parameters and the calibration of camera internal and external parameters can be established. The internal parameters of the camera are calculated by the image of the absolute quadratic curve (IAC). The rotation matrix is calculated by the orthogonal characteristic of the coordinate axis. The translation vector is calculated by the center coordinates of the camera. The calibration results are optimized by using the reprojection method, and the internal and external parameters of the camera can be obtained.

The method of camera calibration using the image of the absolute quadratic curve (IAC) is simple and convenient to use. In this paper, a new target is designed, which is relatively flexible and simple to use. It only needs to shoot several target images under different attitude, and then the calibration work can be finished by calculation, and the final calibration precision is also high. The target can be applied to the occasion in which the camera rotates, and the direction angles of the camera motion can be easily obtained. The application of SLAM in the initialization of visual SLAM is very convenient and free from the constraints of conventional methods. This method provides a train of thought for the application in some special scenes. In this paper, the normalization method is used in data processing, which improves the accuracy of data processing and reduces the influence of coordinate transformation on data. The reprojection method reduces the influence of noise on data. In addition, the method presented in this paper does not need any parameters of the camera in the process of calibration. The distortion coefficient and internal and external parameters of the camera can be obtained by calculating the target image, so it has a wide range of practicability.

REFERENCES

[1] X. Wu, S. Wu, Z. Xing, and X. Jia, "A global calibration method for widely distributed cameras based on vanishing features," *Sensors*, vol. 16, no. 6, p. 838, Jun. 2016.

[2] I. N. Junejo, X. Cao, and H. Foroosh, "Autoconfiguration of a dynamic nonoverlapping camera network," *IEEE Trans. Syst., Man, Cybern. B. Cybern.*, vol. 37, no. 4, pp. 803–816, Aug. 2007.

[3] E. Rosten and R. Loveland, "Camera distortion self-calibration using the plumb-line constraint and minimal Hough entropy," *Mach. Vis. Appl.*, vol. 22, no. 1, pp. 77–85, Jan. 2011.

[4] B. Caprile and V. Torre, "Using vanishing points for camera calibration," *Int. J. Comput. Vis.*, vol. 4, no. 2, pp. 127–139, Mar. 1990.

[5] X.-F. Feng and D.-F. Pan, "A camera calibration method based on plane mirror and vanishing point constraint," *Optik*, vol. 154, pp. 558–565, Feb. 2018.

[6] G. Jiang, H.-T. Tsui, and L. Quan, "Circular motion geometry using minimal data," *IEEE Trans. Pattern Anal. Mach. Intell.*, vol. 26, no. 6, pp. 721–731, Jun. 2004.

[7] R. Furukawa and H. Kawasaki, "Laser range scanner based on self-calibration techniques using coplanarities and metric constraints," *Comput. Vis. Image Understand.*, vol. 113, no. 11, pp. 1118–1129, Nov. 2009.

[8] J. Knight, A. Zisserman, and I. Reid, "Linear auto-calibration for ground plane motion," in *Proc. IEEE Comput. Soc. Conf. Comput. Vis. Pattern Recognit.*, Jun. 2003, p. I.

[9] L. Agapito, E. Hayman, and I. Reid, "Self-calibration of rotating and zooming cameras," *Int. J. Comput. Vis.*, vol. 45, no. 2, pp. 107–127, Nov. 2001.

[10] R. I. Hartley, "Self-calibration of stationary cameras," *Int. J. Comput. Vis.*, vol. 22, no. 1, pp. 5–23, Feb. 1997.

[11] R. Hartley and A. Zisserman, *Multiple View Geometry in Computer Vision*. Cambridge, U.K.: Cambridge Univ. Press, 2003, pp. 134–175.

[12] J. G. Semple and G. T. Kneebone, *Algebraic Projective Geometry*. Oxford, U.K.: Clarendon Press, 1998.

[13] E. Khoramshahi and E. Honkavaara, "Modelling and automated calibration of a general multi-projective camera," *Photogramm. Rec.*, vol. 33, no. 161, pp. 86–112, Mar. 2018.

[14] S. N. Sinha, M. Pollefeys, and L. McMillan, "Camera network calibration from dynamic silhouettes," in *Proc. IEEE Comput. Soc. Conf. Comput. Vis. Pattern Recognit. (CVPR)*, Jun./Jul. 2004, p. I.

[15] R. Rodrigues, J. P. Barreto, and U. Nunes, "Camera pose estimation using images of planar mirror reflections," in *Proc. Eur. Conf. Comput. Vis.*, Berlin, Germany: Springer, 2010, pp. 382–395.

[16] P.-H. Huang and S.-H. Lai, "Contour-based structure from reflection," in *Proc. IEEE Comput. Soc. Conf. Comput. Vis. Pattern Recognit. (CVPR)*, vol. 1, Jun. 2006, pp. 379–386.

[17] P. R. S. Mendonca, K. Y. K. Wong, and R. Cippolla, "Epipolar geometry from profiles under circular motion," *IEEE Trans. Pattern Anal. Mach. Intell.*, vol. 23, no. 6, pp. 604–616, Jun. 2001.

[18] K. Åström, R. Cipolla, and P. J. Giblin, "Generalised epipolar constraints," in *Proc. Eur. Conf. Comput. Vis.* Berlin, Germany: Springer, Apr. 1996, pp. 95–108.

[19] H. Zhang, G. Zhang, and K.-Y. K. Wong, "Auto-calibration and motion recovery from silhouettes for turntable sequences," in *Proc. Brit. Mach. Vis. Conf.*, Jan. 2005, pp. 79–88.

[20] A. W. Fitzgibbon, G. Cross, and A. Zisserman, "Automatic 3D model construction for turn-table sequences," in *Proc. Eur. Workshop 3D Struct. Multiple Images Large-Scale Environ.* Berlin, Germany, Springer, Nov. 1998, pp. 155–170.

[21] H. Zhang and K.-Y. K. Wong, "Self-calibration of turntable sequences from silhouettes," *IEEE Trans. Pattern Anal. Mach. Intell.*, vol. 31, no. 1, pp. 5–14, Jan. 2009.
[22] K. Y. K. Wong, P. R. S. Mendonca, and R. Cipolla, "Camera calibration from surfaces of revolution," *IEEE Trans. Pattern Anal. Mach. Intell.*, vol. 25, no. 2, pp. 147–161, Feb. 2003.
[23] X. Ying, K. Peng, Y. Hou, S. Guan, J. Kong, and H. Zha, "Self-Calibration of Catadioptric Camera with Two Planar Mirrors from Silhouettes," *IEEE Trans. Pattern Anal. Mach. Intell.*, vol. 35, no. 5, pp. 1206–1220, May 2013.
[24] X. Ying, K. Peng, R. Ren, and H. Zha, "Geometric properties of multiple reflections in catadioptric camera with two planar mirrors," in *Proc. IEEE Comput. Soc. Conf. Comput. Vis. Pattern Recognit. (CVPR)*, Jun. 2010, pp. 1126–1132.
[25] K. Forbes, F. Nicolls, G. de Jager, and A. Voigt, "Shape-from-silhouette with two mirrors and an uncalibrated camera," in *Proc. Eur. Conf. Comput. Vis.*, Berlin, Germany: Springer, 2006, pp. 165–178.
[26] A. D. Styliadis and L. A. Sechidis, "Photography-based façade recovery & 3-d modeling: A CAD application in cultural heritage," *J. Cultural Heritage*, vol. 12, no. 3, pp. 243–252, 2011.
[27] K. Mikolajczyk *et al.*, "A comparison of affine region detectors," *Int. J. Comput. Vis.*, vol. 65, nos. 1–2, pp. 43–72, Nov. 2005.
[28] R. Manoranjitham and P. Deepa, "Efficient invariant interest point detector using Bilateral-Harris corner detector for object recognition application," *Multimedia Tools Appl.*, vol. 77, no. 8, pp. 9365–9378, Apr. 2018.
[29] S. Ai, X. Wang, M. Ma, and K. Wang, "A method for correcting non-linear geometric distortion in ultra-wide-angle imaging system," *Optik*, vol. 124, no. 24, pp. 7014–7021, Dec. 2013.
[30] R. I. Hartley, "In defense of the eight-point algorithm," *IEEE Trans. Pattern Anal. Mach. Intell.*, vol. 19, no. 6, pp. 580–593, Jun. 1997.
[31] J. Y. Bouguet. (2004). *Camera Calibration Toolbox for Matlab*. [Online]. Available: http://www. vision. caltech. edu/bouguetj/calib_doc/index. html

WENLEI LIU was born in Yantai, China, in 1988. He received the B.S. degree from the Shandong University of Science and Technology, Qingdao, China, in 2012, and the M.S. degree in Beihang University, Beijing, China, in 2016, where he is currently pursuing the Ph.D. degree.

He mainly studies the high precision visual relative navigation, and also studies the data fusion of multi data sensors to achieve the purpose of cooperative detection and guidance.

SENTANG WU received the Ph.D. degree in dynamics, ballistics, and aircraft motion control systems from National Aviation University, Ukraine, in 1992.

He is currently a Professor of automation science and electrical engineering, and a Ph.D. Tutor with Beihang University, Beijing, China. He is also the Navy Missile Expert with the National Defense Basic Research Institute and a Member of the academic committee. His research interests include the theory and application of nonlinear stochastic systems, computer information processing and control, and aircraft cooperative control, precision, and guidance.

XIAOLONG WU was born in Chengdu, China, in 1988. He received the B.S. degree from Sichuan University, Chengdu, in 2010, and the Ph.D. degree from Beihang University, Beijing, in 2017.

He is currently a Research Associate with the NORINCO Group, Navigation and Control Technology Institute, Beijing. His research interests include the overall design of the guidance and control system for unmanned aerial vehicles, autonomous decision and online planning, and the applications of computer vision.

HONGBO ZHAO was born in Suzhou, China, in 1991. She received the B.S. degree in Beihang University, Beijing, China, in 2016, where she is currently pursuing the Ph.D. degree.

She mainly studies the application of image processing in UAV formation control. She has a deep study of UAV cooperative control.